EACS 2016 – 6th European Conference on Structural Control Sheffield, England: 11-13 July 2016
Paper No. 191

# QUANTIFICATION OF UNCERTAINTY FOR EXPERIMENTALLY OBTAINED MODAL PARAMETERS IN THE CREATION OF A ROBUST DAMAGE MODEL

Gardner, P, Barthorpe, R & Lord, C

Dynamics Research Group, Department of Mechanical Engineering, University of Sheffield, Mappin Street, Sheffield, UK, S1 3JD

pagardner1@sheffield.ac.uk

**ABSTRACT.** Computational modelling is an important method in generating predictive models of engineering systems. These computational models are generally deterministic and therefore often ignore the inherent uncertainty in experimental results. Where the model predictions are to be used for damage identification this lack of uncertainty can lead to less robust classification, as damage states can appear more clearly separated than may be true for experimental data. The approach used in generating damaged state model predictions must therefore identify and quantify the main sources of uncertainties. By quantifying the main sources of uncertainties, a Naive Bayes approach can be used to define decision boundaries that incorporate this uncertainty, improving damage predictions. The combination of the computational model and a Naive Bayes approach will lead to a more detailed and realistic representation of the actual system. In this paper quantification of the uncertainties from modal tests for a prismatic metallic cantilever beam, with different levels of damage, is presented. The main sources of uncertainty are categorised and quantified before being applied to computational models using a Naive Bayes approach. The probability of the likelihood of damage classification is then shown for the inclusion of uncertainty in the damage model, showing the improvement in decision bound and therefore the improvement in the damage model.

**KEYWORDS:** Damage Modelling, Structural Health Monitoring, Uncertainty Quantification

## 1 INTRODUCTION

Structural health monitoring (SHM) is the implementation of a process to monitor the state of a structure with the objective of damage identification. Damage in this context can be broadly defined as a change that adversely affects the structures performance [1]. The process of SHM involves observing a structure over time by acquiring measurements that can be used to determine the current health of the structure, therefore reducing in-service failures and unscheduled maintenance. Rytter first defined the four stages of damage identification as; detection, location, quantification and prognosis [2], where to achieve a higher level of detail requires a more complex SHM approach.

The problem of SHM has currently been approached in two main categories; model driven methods, which use a law-based model and inverse methods [3] [4], and data driven approaches, which are usually based on a statistical representation of the system from data and use pattern recognition and machine learning techniques [5] [6]. Model driven methods, generally based on a finite element (FE) model, use a model updating methodology, whereby certain model parameters are adjusted to reduce residuals between experimental measurements and model predictions [7]. The updated model can then be used to infer damage (detection), as well as its location. These methods can require a large number of parameters, as damage locations are often unknown, and poses issues in correctly parametrising and estimating those parameters for the model [3]. The method generally requires that a single mesh is used and this can lead to discretisation errors [8]. Model driven methods require an accurate understanding of the in-service load and boundary conditions that can be difficult to obtain, and updates to the model may result in the model departing from physical meaning as parameters are adjusted. In addition, these methods also have difficulties incorporating noise and environmental effects. Data driven methods, on the other hand use response data, capturing the complete loading environment (with noise), to establish a normal (undamaged) condition; any deviation from this and damage is then inferred [5]. These methods are statistically based and apply machine learning approaches, either to perform classification, regression or probability density estimation [9] in order to determine the state of the structure.

Data driven approaches do not require a complete understanding of the underlying physics of the structure and it is therefore difficult to achieve prognosis, however examples of this have been achieved [10]. For data driven methods to work most effectively, data is required from all possible damaged states and this is generally not feasible or economically viable. To address these issues, a third method is proposed that uses the development of a damage model for the use in machine learning driven SHM, this therefore allows data from different possible damage states to be generated more feasibly whilst removing the risk of the model departing from the physical meaning. This method uses a law-based model and forward methods to perform damage identification. Lee et al. used this method, with a damage model to train Neural Networks, to predict element damage in bridges whilst observing the effect of model errors [11]. Dua et al. also used FE modelling in a forward mode to generate training data for classifiers, using strains obtained from low velocity impacts on composite plates to train Neural Networks [12]. Yang and Liu used model updating to create an FE model that was subsequently used to generate classification data for Support Vector Machines [13].

This paper looks to develop an FE model capable of simulating damaged-state conditions (herein referred to as a *damage model*) for the purpose of predicting feature values that can be used in a machine learning approach in order to perform damage identification. The steps of the process are as follows: a damage model of potential damage states is validated using experimentally obtained data (and uncertainty is incorporated); damage sensitive features are extracted from the damage model; and these features are used to train a machine learning process. The trained machine learning process is then shown in-service data and subsequently makes predictions of the damage state. A flow of the process is shown in Fig. 1. Many conventional dynamic FE models are deterministic and therefore do not contain uncertainties that are captured in non-deterministic experimental data. This lack of consideration of experimental uncertainties in the FE model can affect the machine learning process, as data that contains slight deviations in the response produced by benign experimental variability, can lead to false identification. The FE model needs to correlate and produce data similar to that obtained experimentally in order to produce the best features for machine learning. Difficulties can also arise in the validation of the FE model against the experimental data. To improve validation of the model and any preceding predictions, the model should incorporate these uncertainties. To this end, experimental uncertainty quantification is performed in order to incorporate experimental uncertainty into the FE modelling process.


Figure 1: A process flowchart for using a damage model in machine learning driven SHM.

There are several approaches to including uncertainties in an FE model. Stochastic FE method is widely used for propagating uncertainties in system parameters such as geometric parameters, Young's modulus and density, by representing them as random variables or fields [14]. Quantification of these propagated uncertainties has also been implemented [15]. Stochastic model updating has been developed to propagate parameters and their Gaussian distributions through a model using Monte-Carlo analysis [16]. However the parameter uncertainties and their statistical distributions may not be available prior to modelling for both these methods and may be harder to obtain than simply testing the structure. Griffith and Carne quantified experimental uncertainty in a modal test of a wind turbine blade by looking at individual sources of experimental uncertainty [17]. They categorised the force level, excitation location and algorithm as sources of aleatoric uncertainty (inherent variability). Furthermore, they categorised the instrumentation cable effects and ambient environment as sources of epistemic uncertainty (lack of knowledge). They then quantified the contribution from each uncertainty type.

In this paper the quantification of several sources of uncertainty has been conducted and their variances used in constructing a Naive Bayes classifier. The approach is shown to be more robust when the distributions from different damage states overlap and therefore will be a more robust method of using a damage model for machine learning driven SHM.

The outline of the paper is as follows. Section 2 outlines the experimental work and the quantification of uncertainties from various sources. In Section 3 the FE modelling approach is shown along with the model's correlation with the experimental results. Lastly, in Section 4 a demonstration of the inclusion of uncertainties in a Naive Bayes classifier is presented. Conclusions and areas for further research are outlined in Section 5.

## 2 CANTILEVER BEAM EXPERIMENT

Experiments were conducted to quantify the uncertainty present in testing a cantilever beam for various damage states. A damage state is defined here as the introduction of damage via a saw cut, at different lengths, as a proxy representation of an open crack. The first six bending modes of the structure were obtained for each damage state. The experiments quantified uncertainty from several sources: the algorithm used to extract the modal data, the ambient environmental effects, changes in the boundary condition, the change in the beam being used (geometric and material properties - nominally the same), as well as a grouping of miscellaneous causes of uncertainty.

### 2.1 Experimental Set-up

Five uniformly prismatic cross-section cantilever beams made from Aluminium Grade 6082 were used in the experiments. Nominal physical and geometrical properties of these aluminium beams are shown in Table 1.

Table 1: Geometric and material properties of the beams used in the experiment.

| **Beam Properties** | Length, $l$ | Width, $w$ | Thickness, $t$ | Young's Modulus, $E$ | Density, $\rho$ | Poisson's Ratio, $\nu$ |
|---|---|---|---|---|---|---|
| **Values** | 655mm | 25.5mm | 6.5mm | 71GPa | 2700kg/m$^3$ | 0.33 |

The beams were fixed at one end to provide a fixed-free boundary condition. A 100mm clamp plate, $l_c$, was fastened to a heavy steel block that in turn was attached to a rigid table. Each fastener was tightened to a torque of 20Nm. This was repeated for each beam to ensure consistency in the boundary condition. A schematic of the experimental test set-up is shown in Fig. 2.

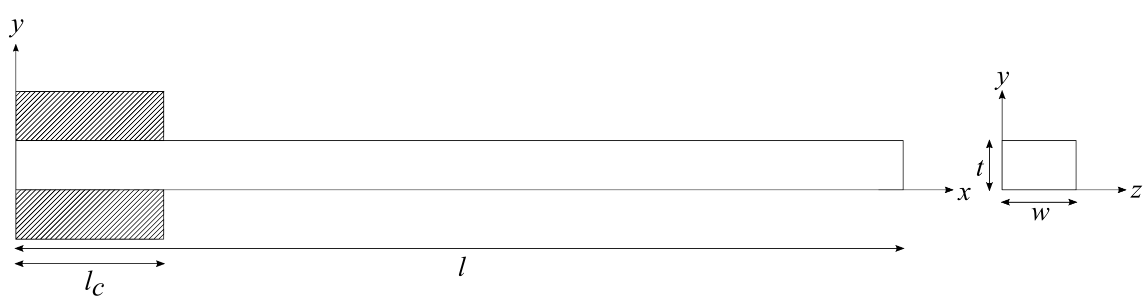


Figure 2: A schematic of the experimental set-up for the fixed-free beam.

### 2.2 Experimental Methodology

Modal testing was used to analyse the beams for the first six bending modes. Two accelerometers were placed at 225mm and 475mm from the right hand edge of the clamp in Fig. 2, this was to avoid the node points of the first six flexible modes. A roving impact hammer was used to excite the structure in the $y$-direction. Acquisition and analysis of the data was performed using a LMS Test.Lab system with a bandwidth of 6400Hz, 4096 spectral lines and a resolution of 0.78Hz and an exponential response window.

To obtain the mode shapes, each beam was divided along the length into twelve impact points each 50mm apart and an average frequency response function (FRF), using the *H1* estimator, was obtained from fifteen repeated experiments. A damage location of 175mm from the right hand edge of the clamp in Fig 2 was used, as shown in Fig. 3. The beams were tested in the undamaged state before damage was added. A saw cut was made in the $z$-direction in increments of 2.5mm up to 20mm. The excitation procedure was repeated five times for each damage state. The repetition aimed to quantify the uncertainty present in the excitation and acquisition procedure. LMS PolyMAX was used to extract the modal data from the FRFs.

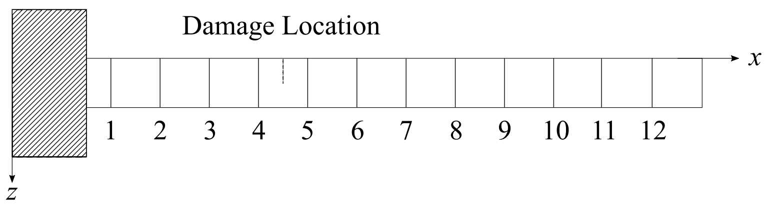


Figure 3: A schematic of the impact points and damage location.

For each of the five beams in the undamaged scenario, the beam was removed from the boundary condition and reattached with a 20Nm torque on each fastener. This was to quantify the uncertainty present in a change in boundary condition. The temperature was also recorded for each test although the structure was in ambient conditions.

### 2.3 Sources of Experimental Uncertainty

Uncertainties are present throughout the experimental processes; from the experimental set-up, the data acquisition methodologies, measurement choices, as well as the data analysis processes. Several sources of uncertainty were identified in the cantilever experiment; these can be categorised for this example into the aleatoric and epistemic categories as shown in Table 2.

Table 2: Categorised sources of uncertainty from the cantilever beam experiment.

| Aleatoric | Epistemic |
|---|---|
| • Ambient Environment | • Boundary Condition<br>• Different Beam<br>• Excitation Force<br>• Excitation Location<br>• Instrumentation Cable Effects<br>• Modal Identification Algorithm<br>• Sensor Effects |

Uncertainties due to the excitation force, excitation location, instrumentation cable and sensor effects have been grouped into a miscellaneous uncertainty group, this is due to their effects being relatively small when compared to the other uncertainty sources. For each source of uncertainty a variance has been calculated. Initially variances were calculated for the modal frequency, $\omega$, as shown in Table 3. However when selecting a feature for machine learning the normalised percentage difference, $\Delta\omega$, of the modal frequency is used as it is a more damage sensitive feature. As shown in Table 4 the variances generally decrease once the percentage difference is used due to the normalisation, this shows that by using the percentage difference the effects of uncertainty are reduced. Uncertainties from each source have been assumed to be uncorrelated, and therefore the variance of each source can be summed for a total variance due to uncertainty sources as shown in Table 4.

Table 3: Variances of modal frequency, $\omega$, associated with each source of uncertainty.

| **Uncertainty Source** | **Mode 1** | **Mode 2** | **Mode 3** | **Mode 4** | **Mode 5** | **Mode 6** |
|---|---|---|---|---|---|---|
| Ambient Environment | 0.000743 | 0.014212 | 0.112681 | 0.378093 | 1.372767 | 5.412003 |
| Boundary Condition | 0.000518 | 0.010440 | 0.074584 | 0.498570 | 0.522381 | 5.777136 |
| Different Beam | 0.000626 | 0.011928 | 0.094650 | 0.317856 | 1.151764 | 4.582419 |
| Modal Identification Algorithm | 0.000003 | 0.028325 | 0.072035 | 0.156642 | 0.303469 | 0.415891 |
| Miscellaneous | 0.000044 | 0.000547 | 0.003543 | 0.014861 | 0.044483 | 0.532502 |

Table 4: Variances of the percentage difference of modal frequency, $\Delta\omega$, associated with each source of uncertainty.

| **Uncertainty Source** | **Mode 1** | **Mode 2** | **Mode 3** | **Mode 4** | **Mode 5** | **Mode 6** |
|---|---|---|---|---|---|---|
| Ambient Environment | 0.029641 | 0.013359 | 0.014100 | 0.011391 | 0.015870 | 0.028736 |
| Boundary Condition | 0.018482 | 0.009391 | 0.008413 | 0.014786 | 0.005822 | 0.028533 |
| Different Beam | 0.024986 | 0.011210 | 0.011838 | 0.009575 | 0.013314 | 0.024329 |
| Modal Identification Algorithm | 0.000099 | 0.025450 | 0.008098 | 0.004636 | 0.003418 | 0.002048 |
| Miscellaneous | 0.001631 | 0.000499 | 0.000418 | 0.000441 | 0.000507 | 0.002785 |
| Summed Variance | 0.074839 | 0.059910 | 0.042866 | 0.040829 | 0.038931 | 0.086431 |

Data from the undamaged state was used to calculate the variances in Table 3 and 4. The uncertainty due to the ambient environment was measured from an average of the five tests of five observations. The variance associated with the change in boundary condition was calculated from 25 observations obtained from the beam in both the initial and replaced boundary condition. A total of 125 observations, for each of the five beams, were used in calculating the uncertainty associated with using a different beam. The variance due to the modal identification algorithm was calculated from 42 observations of data obtained by selecting multiple possible stable poles in LMS PolyMAX. The miscellaneous source of uncertainty was quantified from the five test repeats, five observations, and an average was taken for the five beams.

The main sources of uncertainty from both Table 3 and 4 are the ambient environment effects and the change in boundary condition. The main source of uncertainty does however change for each mode as shown by the summed variances and modes one and six have the highest degrees of uncertainty, although the variances for each mode are relatively low.

## 3 FINITE ELEMENT MODEL

Models of the beam under different damage scenarios were created using FEs in the commercial solver ANSYS. Friswell and Penny have categorised three main ways of modelling a crack [18]; local stiffness reduction, discrete spring models and complex models in two or three dimensions. This work uses geometric modelling in two dimensional models using a second order shell element (SHELL281). For each experimental damage scenario a mesh refined FE model was created with the damage modelled as a removal of geometry, the width (in the beams $x$ direction) of the damage being 1mm (the same as the width of the saw cut in the experiment). The first six bending modes were obtained for each FE damage state and the modal assurance criterion (MAC) was used to check that the modal frequencies were assigned to the same bending mode. The normalised percentage difference of the modal frequencies were then calculated.

### 3.1 Model Correlation

Figure 4 shows the modal frequency percentage difference for both the experimental and computational results. The experimental results for each beam are displayed along with the mean, $\mu$ and three standard deviations, $3\sigma$ and show a good visual correlation with the computational results. However in the FE model the fourth mode starts to show combined torsion and bending modes after a damage depth of 17.5mm, this may account for the differences between the experimental and FE model results. The maximum difference in absolute modal frequencies between the FE model and the average experimental results is approximately 5%. For the relative errors $\Delta\omega_{1-6}$, the root mean square (RMS) error between the mean experimental data and the FE model predictions across the full damage range was 0.043. While formal model validation was not pursued for this study, it was deemed that a good degree of correlation between FE and experiment had been achieved, as might be expected for a comparatively simple structure and damage case. It should be highlighted that one of the benefits of adopting a geometrically accurate damage model is that the damage extent (the depth of cut in this case) is explicit, which is not the case when applying local stiffness reduction to simulate damage.

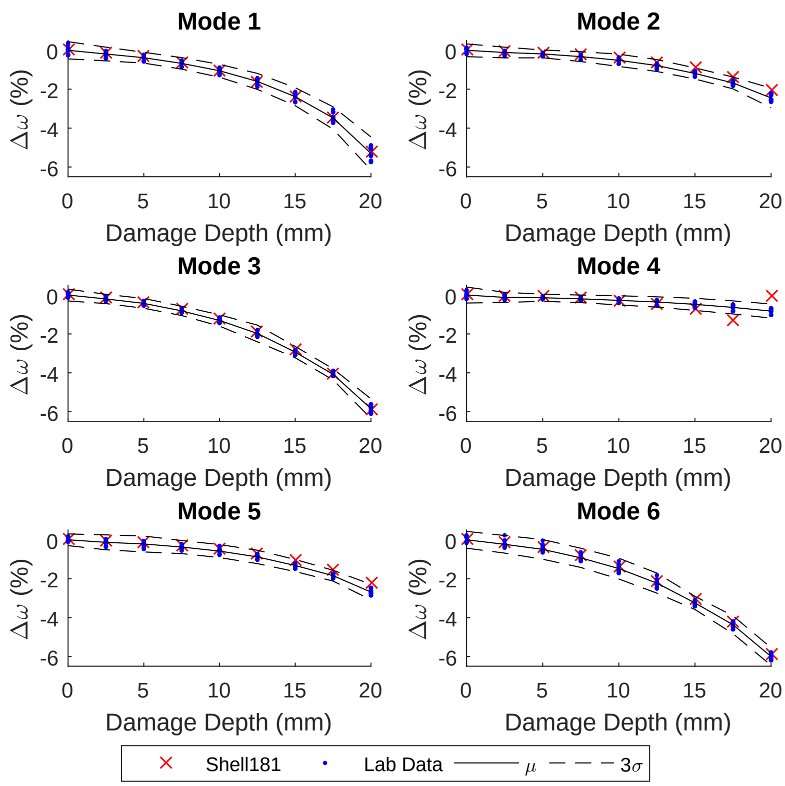


Figure 4: Comparison of percentage difference of modal frequency for experimental and computational results.

## 4 CLASSIFICATION

To achieve the first stage in SHM, damage detection, classification methods are generally used. These methods involve defining a damage class and a decision boundary between the damaged and undamaged data, and subsequently using this boundary in predicting the class of new data. Figure 5 shows the experimental data and distributions for each damage state as well as the damage model predictions combined with the experimental uncertainties; where all distributions are assumed to have a normal Gaussian distribution. If an undamaged class was set to only include data from the 0mm damage state a decision boundary from the FE results may create a hard bound, one that assigns with complete certainty whether new data is either damaged or undamaged. However, as shown in Fig. 5 data in the 0mm, 2.5mm and 5mm damage states all overlap and a hard bound from the FE model could result in misclassification of data when in-service data is introduced. The inclusion of experimental uncertainties therefore provides a more realistic representation of the real world scenario and can be used to train a better soft decision boundary, one that accounts for the overlap by assigning probabilities to new data near a bound.

Figure 5 shows that the deterministic FE damage model can be corrected to incorporate experimental uncertainties. Additionally Fig. 5 displays a deviation between the FE model and experimental results, showing evidence of a bias in the FE model results. While not pursued as part of this study, this bias may be overcome by using Bayesian calibration methods as outlined by Kennedy and O'Hagan [19].

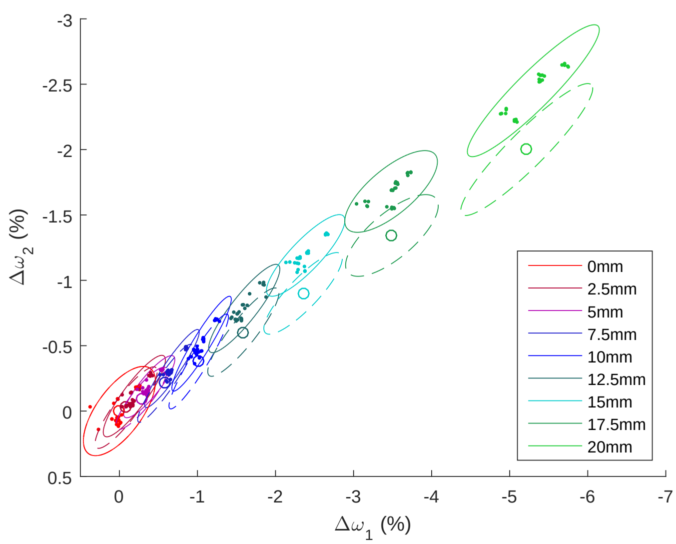


Figure 5: Comparison of damage state distributions for mode 1 and mode 2 for both the experimental results (· -) and FE model prediction with combined uncertainty (o - -).

A soft decision bound can be created using a Naive Bayes approach. The probability of the likelihood, of the data given the class, is assumed to be from a multivariate normal Gaussian distribution as shown in Eq. (1).

$$p(X|C_{UD}) = \prod_{n=1}^{N} \frac{1}{\sqrt{|\mathbf{\Sigma_{UD}}|\,(2\pi)^6}} \exp\left[\frac{1}{2}\left(\mathbf{x}-\mu_{\mathbf{UD}}\right)^T \mathbf{\Sigma_{UD}}^{-1}\left(\mathbf{x}-\mu_{\mathbf{UC}}\right)\right] \tag{1}$$

Where $X$ is the FE data for each damage state, $C_{UD}$ is the undamaged class, $N$ is the number of damage states, $\mathbf{\Sigma_{UD}}$ the covariance matrix of the undamaged class that includes the uncertainty sources, $\pi$ is the mathematical constant Pi, $\mu_{\mathbf{UD}}$ is the mean of the undamaged class and $^T$ is the Hermitian transpose of a matrix. Figure 6 shows a comparison of the probability of the likelihood for a hard and soft decision boundaries assuming that the undamaged class contains only data from the 0mm damage state. This shows that the addition of uncertainty can improve decisions made where their is overlap between different classes.

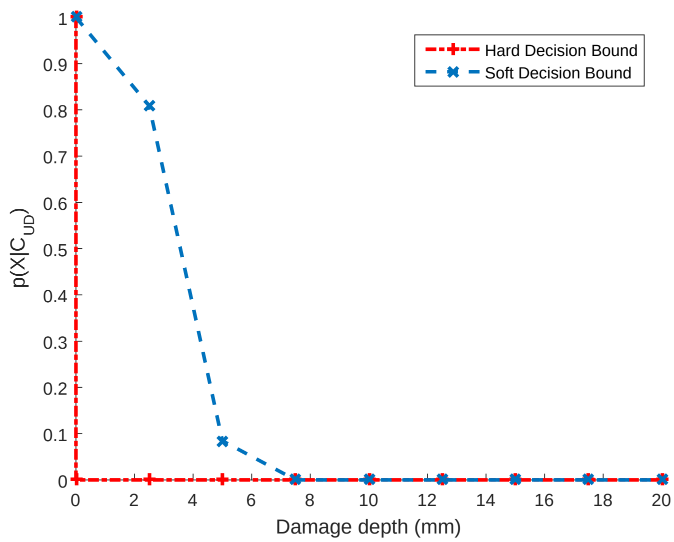


Figure 6: Comparison of the probability of the likelihood for a hard and soft decision bound assuming the undamaged case is a 0mm saw cut.

## 5 CONCLUSIONS

In this paper quantification of uncertainty sources from experimental modal testing has been presented. Uncertainties were considered from several sources; from the ambient environment, the boundary condition, different beams used, the modal identification algorithm as well as miscellaneous sources. It has been shown that when using the percentage difference of modal frequencies that uncertainties due to different sources generally decrease, showing that it is a good feature for reducing the effects of uncertainties in machine learning. The main sources of uncertainty were due to ambient environment effects and the change in boundary condition; both of these sources are difficult to model directly and therefore need to be statistically incorporated.

An FE damage model has been produced that shows good agreement with the experimental data. It assumes a deterministic response of the system which can pose problems in performing damage identification with non-deterministic in-service data. The quantified uncertainty sources have been incorporated into the FE model but a bias has been shown between the FE and experimental results. A soft decision bound has been created from the FE model predictions using a Naive Bayes approach that incorporates the experimental uncertainties. This probability can be used to distinguish the probability of data belonging to a damage class in areas of overlap between damage state distributions.

Further work is suggested to remove the bias from the FE damage model using Bayesian calibration techniques. Full validation of the damage model using appropriate validation metrics is also suggested to ensure that the damage model is appropriate for damage identification either by classification or regression. An informative prior such as a Bernoulli distribution can also be used to find the posterior for the Naive Bayes approach.

## REFERENCES

[1] Farrar, C. R. & Worden, K., An Introduction to Structural Health Monitoring, *Philosophical Transactions: Mathematical, Physical and Engineering Sciences*, 2007; **365**, pp. 303-315

[2] Rytter, A., Vibration Based Inspection of Civil Engineering Structures, *PhD Dissertation University of Aalborg*, 1993; **R9314**

[3] Friswell, M. I. & Mottershead, J. E., Inverse Methods in Structural Health Monitoring, *Key Engineering Materials*, 2001; **204-205**, pp. 201-210

[4] Friswell, M. I., Damage Identification using Inverse Methods, *Philosophical Transactions of the Royal Society of London A: Mathematical, Physical and Engineering Sciences*, 2007; **365**, pp. 393-410

[5] Worden, K. & Manson, G., The application of machine learning to structural health monitoring, *Philosophical Transactions of the Royal Society of London A: Mathematical, Physical and Engineering Sciences*, 2007; **365**, pp. 515-537

[6] Farrar, C. R. & Worden, K., *Structural Health Monitoring: A Machine Learning Perspective* Wiley, 2013

[7] Friswell, M. I. & Mottershead, J. E., Physical Understanding of Structures by Model Updating, *International Conference on Structural System Identification*, 2001; pp. 81-96

[8] Mottershead, J. E., Link, M., Friswell, M. I., The sensitivity method in finite element model updating: A tutorial, *Mechanical Systems and Signal Processing*, 2011; **25**, pp 2275-2296

[9] Cherkassky, V. & Mulier, F., *Learning from Data, Concepts, Theory and Methods*, Wiley, 1998

[10] Fuentes, R., Cross, E., Halfpenny, A., Worden, K. & Barthorpe, R. J., Autoregressive Gaussian Process Regression for Structural Damage Detection, *International Conference on Noise and Vibration Engineering*, 2014; **711**

[11] Lee, J. J., Lee, J. W., Yi, J. H., Yun, C. B., & Jung, H. Y., Neural Networks-Based Damage Detection for Bridges Considering Errors in Baseline Finite Element Models, *Journal of Sound and Vibration*, 2005; **280**, pp. 555-578

[12] Dua, R., Watkins, S. E., Wunsch, D. C., Chandrashekhara, K., Akhavan, F., Detection and classification of impact-induced damage in composite plates using neural networks, *Proceedings of the International Joint Conference on Neural Networks*, 2001; **1**, pp. 681-686

[13] Yang, Y. & Liu T., Application of Support Vector Machine in Structure Damage Identification, *Proceedings of the International Conference on Information Engineering and Computer Science*, 2009; pp.1-3

[14] Sachdeva, S. K., Nair, P. B. & Keane, A. J., Comparative study of projection schemes for stochastic finite element analysis, *Computer Methods in Applied Mechanics and Engineering*, 2003; **195**, pp. 2371-2392

[15] Adhikari, S., Friswell, M. I., Lonkar, K. & Sarkar, A., Experimental case studies for uncertainty quantification in structural dynamics, *Probabilistic Engineering Mechanics*, 2009; **24**, pp. 473-492

[16] Mares, C., Mottershead, J. E., Friswell, M. I., Stochastic model updating: Part 1 - theory and simulated example, *Mechanical Systems and Signal Processing*, 2006, **20**, pp. 1674-1695

[17] Griffith, D. T. & Carne, T. G. Experimental Uncertainty Quantification of Modal Test Data, *Proceedings of the 25th International Modal Analysis Conference*, 2007

[18] Friswell, M. I. & Penny, J. E. T., Crack Modeling for Structural Health Monitoring, *Structural Health Monitoring*, 2002; **1**, pp. 139-148

[19] Kennedy, M. C., O'Hagan, A., Bayesian Calibration of Computer Models, *Journal of the Royal Statistical Society. Series B (Statistical Methodology)*, 2001; **63**, pp. 425-464